

EFFECT OF PUMPING TYPES ON OPTICAL PATH DIFFERENCE IN ND:YAG LASER ROD

Zahraa Mohamed Ali Kamil
University of Technology

ABSTRACT:- The finite element method has been used successfully to determine the temperature distribution throughout Nd:YAG laser rod subjected to one end power pumping cooled by water from the longitudinal side. Displacement, strain and stress are obtained numerically depending on the temperature distribution using Hook's law. The influence of two types of pumping methods on temperature, displacement, strain and stress is obtained. The optical path difference is obtained and compared with a previously published experimental data and a good agreement has been found. Some conclusions are drawn; Gaussian beam pumping causes higher temperature distribution more than Top hat beam pumping at and near the center of the rod, which may cause higher optical path difference there. Even Top hat beam pumping causes some high tensile hoop stress, it may be a better choice while designing laser system since it results in low optical path difference.

Keywords:- Thermal lensing, Gaussian pumping method, Top hat pumping method, Optical path difference, Thermal stress, Nd:YAG laser rod.

1- INTRODUCTION

One of the main problems in a high solid state laser system is the heat that could be generated through the process of laser generation, which must dissipate efficiently, if high laser power output is required. Advance Nd:YAG laser applications which require increasingly higher average output power necessitate operating near the stress-fracture limit, i.e., a regime in which output power is limited by the possibility of material fracture arising from thermally induced stresses in the laser **medium**^(1,2). At average powers below the stress-fracture limit, heating also leads to thermo-optic aberrations, lensing, and birefringence that reduce the efficiency of laser operation, decrease the output beam quality, and change the

resonator stability with pump power⁽³⁾. The fractional thermal load is defined as the fraction of the absorbed pump power that is converted into heat, which contributes to the aforementioned determinate effects. Thermal lensing effects and aberrations are particularly strong at the pump face of end pumped solid- state lasers. Inhomogeneous local heating and non uniform temperature distribution in the laser crystal lead to a degradation of the beam quality owing to the highly aberrated nature of the thermal lens. With the availability of high-power diode lasers, end pumping, or longitudinal pumping, of laser crystals has become a very important technology.

In this work finite element method has been used to determine temperature distribution, strain and stress associated with different end pumping methods at various pumping radii from which optical path difference (OPD) is obtained, which stand for the variation in the optical path length of different rays in an optical system. In theory, perfect systems show no optical path difference; in practice all systems exhibit small differences: these may cause phase variations and decreases the output beam quality, so efficient laser system must work with minimum optical path difference to enhance beam quality.

The following section discuss the theory on which the analysis of temperature distribution where the axis- symmetry based on Fourier's equation is used with two types of the end pumping and different types of thermal boundary conditions. In Section III, the finite element analysis to determine temperature, thermal strain and stress is discussed, which is used to determine the optical path difference. In Section IV, the results of the computer program that is used in this work are verified by experimental data to ensure its accuracy. The results obtained from this program are discussed in Section V where finally, a Top hat beam seems to cause less optical path difference than Gaussian beam even if it may result in some higher tensile hoop stresses.

2- THEORY

2.1 Partial differential equation and boundary conditions

The partial differential equation that covers the axis-symmetric domain of laser rod can be written as⁽³⁾:

$$\frac{1}{r} \left[k \frac{\partial}{\partial r} \left(r \frac{\partial T}{\partial r} \right) \right] + k \frac{\partial^2 T}{\partial z^2} + Q(r, z) = 0 \quad (1)$$

where T is the temperature distribution in $^{\circ}C$, $Q(r, z)$ is the heat source density that is function of the pump power density, r and z are the radial and longitudinal coordinates, k is the

thermal conductivity of Nd:YAG laser rod that's assumed to be temperature dependent and can be determined by⁽⁴⁾:

$$k = 1.9 \times 10^8 [\ln(5.33T)^{-7.14}] - 33100 / T \quad (2)$$

Tested laser rod has outside diameter D_1 of 9.5 mm, the length of the laser rod L is 20mm, also convection heat transfer coefficient h at the surface ends is assumed to be 50 (W/(m².K)). The rod outer boundary is held at a constant temperature of 25 °C and the rod is assumed to freely expand in all directions. The rod mount, described in⁽⁵⁾, is consistent with these boundary conditions. Also for special diode protection and cooling to each diode, it operates at a temperature which yields the highest absorption of the pump light. Under these conditions, 96% of the incident pump power can be absorbed in the active medium.

2.2 Source density heat

Two types of possible pumping method can be tested; Gaussian and Top hat beam distribution, they will cause heat generation through the laser medium. For Gaussian beam distribution, the heat generation through the laser medium ($\mathcal{Q}(r, z)$ in W/m³) can be written as⁽⁶⁾:

$$\mathcal{Q}(r, z) = \frac{2Q\mu \exp\left(\frac{-2r^2}{w_o^2}\right) \exp(-\mu z)}{\pi w_o^2 [1 - \exp(-\mu L)]} \quad (3)$$

where $Q = \eta P$, η is thermal factor, P absorption power(W), w_o waist radius (m), μ absorption coefficient (3.50 cm⁻¹), L is length of laser rod (m). For uniform power distribution through the beam (Top hat), the heat generation through the laser medium can be written as⁽⁷⁾:

$$\mathcal{Q}(r, z) = \frac{Q\mu \exp(-\mu z)}{\pi a^2 [1 - \exp(-\mu L)]} \quad r \leq a \quad (4)$$

where heat generation is zero elsewhere (i.e. the heat generation vanishes when the radius is greater than the pumping beam radius a).

3- FINITE ELEMENT FORMULATION

3.1 Thermal analysis

Equation (1) is discretized in axis-symmetry spatial dimensions and solved using the weak formulation and Galerkin procedure⁽⁸⁾. Figure 1 shows half of the studied region it shows 886 triangular axis-symmetry elements that contain 491 nodes, which is used in the

analysis where z refers to axial direction and r to radial dimensions. A computer program is created using VB6 coding to follow the procedure of predicting the temperature distribution through the domain and the subsequent nodal displacement, strain and thermal stress in the region of interest. The same mesh which has been used to predict temperature distribution is used in mechanical analysis even if different mythologies are implemented.

3.2 Thermal stress analysis

The inhomogeneous heat source produced by the two types of side end pumping causes a non-uniform temperature distribution, resulting in the thermal stress in the laser rod.

The finite element method is adopted to calculate the thermal stress distribution. From Hooke's law, the equation for calculating the stress and strain components in the rod is used where the displacement is obtained first from which thermal strain can be calculated and finally thermal stress is predicted, the procedure is clearly followed by reference 9 and the reader is advised to read the extensive discussion of thermal stress determination followed by the above reference for further information. It is generally admitted that fracture occurs when the maximum hoop (tangential) stress anywhere in the rod exceeds its yielding tensile stress which is found to be in the range of 124 to 255 MPa⁽³⁾. The latter depends on both the fracture toughness of the material and its surface flatness. These aspects have been studied in detail by⁽¹⁰⁻¹²⁾. The fracture tensile strength for Nd:YAG material is known to be equal to 137.88 MPa⁽¹³⁾, which is used in this work.

Note that the thermal expansion coefficient of Nd:YAG laser rod, α , which is used to determine thermal strain, is treated as temperature-dependent and can be expressed as follows⁽¹³⁾:

$$\alpha(T) = -1.78 \times 10^{-6} + 3.3 \times 10^{-8} T \quad (5)$$

The present study uses a mean or weighted-average value of α , such that:

$$\bar{\alpha} = \frac{\int_{T_{ref}}^T \alpha(T) dT}{T - T_{ref}} \quad (6)$$

where T_{ref} is the temperature at which cooled laser rod surface is hold on, which is assumed to be 25 °C.

3.3 Optical path difference

A valuable means to quantify the optical properties of thermally loaded laser material is the optical path difference (OPD) which denotes the optical path differences between the propagation in air and the path differences between undisturbed and the disturbed rod (heated rod). For a paraxial coherent beam propagating in the z direction over an infinitesimal distance dz , the differential OPD is given by⁽¹³⁾, where it is assumed the unpumped surface is coated to be highly reflective, i.e. being used as a mirror. Neglecting the contribution from thermal stress induced birefringence which is small for most cases⁽²⁾, the OPD can be expressed as

$$OPD(r) = 2 \left(\int_L \frac{\partial n}{\partial T} T(r, z) dz + \int_L n \varepsilon_{zz} dz \right) \quad (7)$$

where n is the refractive index of the rod and ε_{zz} is the longitudinal strain.

Even if the optical path difference(OPD) is well known in the optical science, it can verify the thermal and mechanical analysis used in this work since its terms depend on temperature distribution, variation in refractive index with temperature and strain distribution.

4- VALIDATION

A program has been tested with a previously published experimental data. The value of center to edge OPD has been obtained numerically using this program. The result from the created program is in order of $2.13 \mu m$ which is very near to a value of $2.15 \mu m$ as obtained experimentally by⁽¹³⁾ (i.e. 0.9% allowance).

5- RESULTS AND DISCUSSION

The numerical simulation has been used to obtain temperature distribution, displacement, strain and stress across continuous pumped Nd:YAG laser rod of 1064 nm (in the 4th system level), its rod was end pumped from one side and it has been tested with absorption power ranging from 20 to 100 W for radius pumping ratio of 1/2, 1/3, and 1/4, for both Top hat and Gaussian beam pumping.

As an example, the temperature distribution at 100W absorption power and radius pumping ratio of 1/2 is shown in Fig 2. It shows that Gaussian beam pumping will increase the temperature distribution more than that for Top hat beam especially, at the central portion of the rod. This will cause more intense compressive hoop stress there, this compressive hoop tensile stress is not the one that may cause fracture since compressive failure stress is 5~6

times larger than tensile failure stress for crystal material so the fracture caused by the tensile hoop stress is more probably to happen at the outside portion of the rod especially at facet of the rod. It may reach 114.5MPa for Top hat beam and about 113 MPa for Gaussian beam.

The entire distribution of hoop stress through laser rod is shown in Fig3. It shows that the compressive hoop stress in the central portion of the rod is much higher than that of Top hat beam pumping and this is not the case for the outer portion of the rod where Top hat pumping will cause some increase in the tensile hoop stress seen there. This is also shown in Fig4 for various pumping power levels. Fig5 shows the strain through the laser rod at pumping ratio of $\frac{1}{2}$ and pumping power of 100W. An intense strain, which results from high temperature is shown, which may explain the increase in OPD for Gaussian beam is more than that of Top hat pumping beam.

A basic definition of OPD is that it stands for the variation in the optical path length of different rays in an optical system. The aim is to reduce the value of OPD, Top hat beam stands for this advantage rather than Gaussian beam. By testing the terms of OPD equation which consist of temperature term that stands for variation in the refraction index and the second term that stands for influence of strain, it shown that both aforementioned factors have highest value in Gaussian pumping beam compared with that of Top hat beam, so one expects high OPD for Gaussian beam as shown in Fig 6. As pumping power increases, OPD will increase, since the temperature and the strain may increase also.

If a choice has to be made while designing laser system a Top hat beam is a better choice from the site of optics even if it may reach failure stress before Gaussian beam at high power level absorption.

6- CONCLUSIONS

The finite element analysis has been used successfully to predict the temperature distribution, strain and stress through laser rod. The results of the created program were compared with the values of previously published experimental data for OPD, a good agreement has been found.

Some conclusions have been obtained:

1. Gaussian beam pumping causes higher temperature distribution than a Top hat beam at and near the center of the rod which may cause higher OPD since the two important parameters that that effect OPD depend mainly on temperature distribution and its effects.

2. Even Top hat beam pumping causes some high tensile hoop stress as shown in fig 4, it may be a better choice in designing laser system as a pumping beam style since it results in low OPD which indicated in fig 6.

7- RERERENCES

1. J. M. Eggleston, T. J. Kane, K. Kuhn, J. Unternahrer, and R. L. Byer, 1984, "The slab geometry laser-Part I: Theory," IEEE J. Quantum Electron., vol. QE-20, pp. 289-301.
2. J. L. Emmett, W. F. Krupke, and W. R. Sooy, Sept. 1984, "The potential of high-average-power solid-state lasers," LLNL, Livermore, CA, Rep. UCRL-53571, pp. 1-51.
3. W. Koechner, 2006, 6th edition, "Solid-state laser engineering," Springer Series in Opt. Sci., USA, pp. 423-426.
4. Steve C. Tidwell, Jonathan F. Seamans, Mark S. Bowers, and Ananda K. Cousins, April 1992, "Scaling CW diode-end-pumped Nd : YAG lasers to high average powers," , IEEE Journal of Quantum Electronics, vol. 28, no. 4, pp. 997-1009.
5. D.C. Brown, 1998, "Nonlinear thermal and stress effects and scaling behavior of YAG slab amplifiers," IEEE Journal of Quantum Electronics, vol. 34, no. 12, pp. 2393-2402.
6. J. Frauchiger, Peter Albers, and Heinz P. Weber, 1992, "Modeling of thermal lensing and higher order ring mode oscillation in end-pumped CW Nd: lasers," IEEE Journal of Quantum Electronics, vol. 28, no. 4, pp. 1046-1056.
7. Ananada K. Cousins, 1992, "Temperature and thermal stress scaling In finite-length end-pumped laser rods," IEEE Journal of Quantum Electronics, vol. 28, no. 4, pp. 1057-1069.
8. R. W. Lewis, K. Morgan, H. R. Thomas, K. N. Seetharamu, 1996, "The finite element method in heat transfer analysis," John Wiley & Sons Ltd., Chi Chester, U.K, p.p. 13-14.
9. S.S. Rao, 2004, fourth edition, "The finite element method in engineering," Elsevier Science and Technology Books, p.p. 279-305.
10. M. Sunar, B.S. Yilbas K. Boran, 2006, "Thermal and stress analysis of a sheet metal in welding," Journal of Materials Processing Technology, vol. 72, pp. 123-129.
11. Ovais U. Khan, B.S. Yilbas, 2004, "Laser heating of sheet metal and thermal stress development," Journal of Materials Processing Technology, vol. 155-156, pp. 2045-2050.
12. J. Marion, 1985, "Strengthened solid-state laser materials," Applied Physics Letters, vol. 47, no. 7, pp. 94-96.

13. C.Pfisther, 1994,"Thermal beam distortions in end-pumped Nd:YAG,Nd:GSGG, and Nd:YLF rods," IEEE Journal of Quantium Elelectronics, vol.30,no.7,pp.1605-1614.

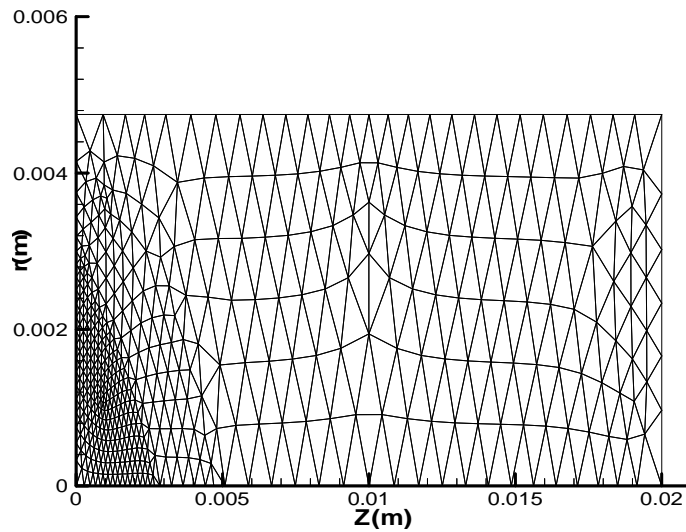


Fig.(1):Mesh and laser rod dimensions in finite element solution.

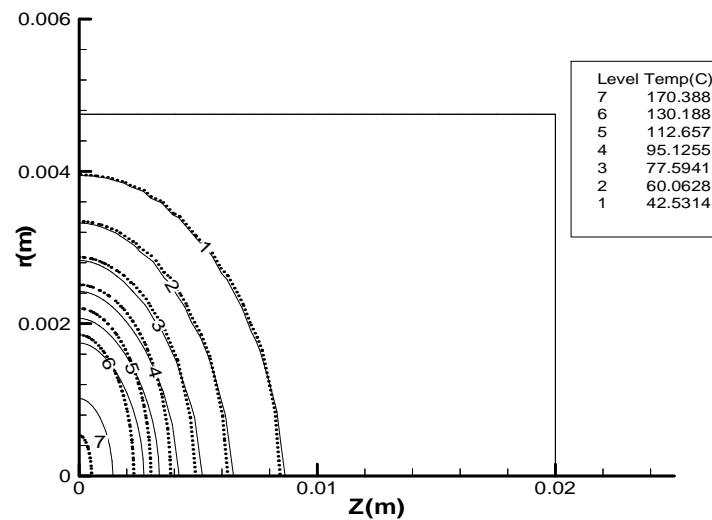


Fig.(2): Temperature distribution in laser rod at absorption power of 100W and radius pumping ratio of 1/2, solid line for Gaussian beam pumping , dashed line for Top hat beam pumping.

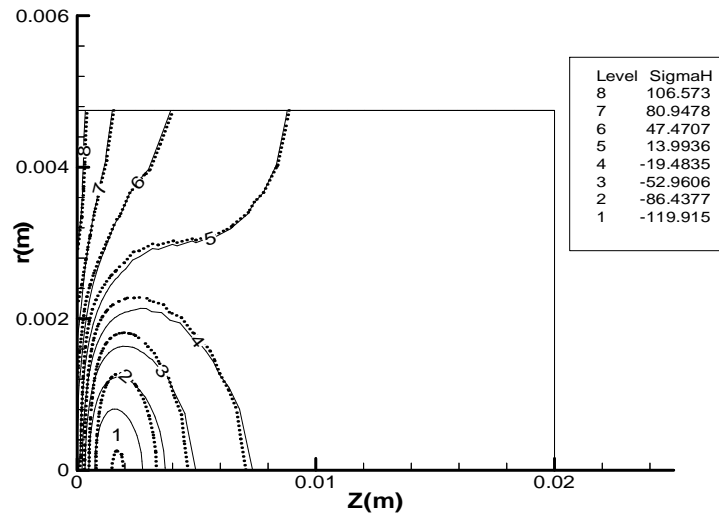


Fig.(3): Hoop stress distribution in laser rod in MPa at absorption power of 100W and radius pumping ratio of 1/2, solid line for Gaussian beam pumping , and the dashed line for Top hat beam pumping.

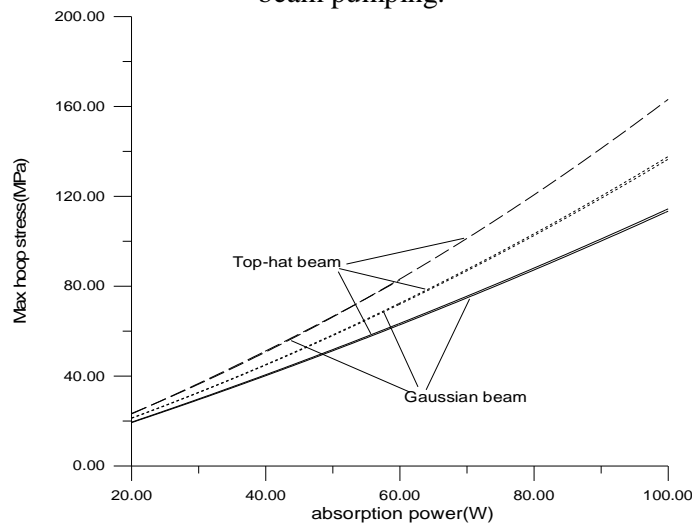


Fig.(4): Variation in maximum hoop stress with absorption power at different levels of pumping radius, and different pumping beam profiles, solid line for pumping radius=1/2,dot line for pumping radius=1/3, dashed line for pumping radius=1/4.

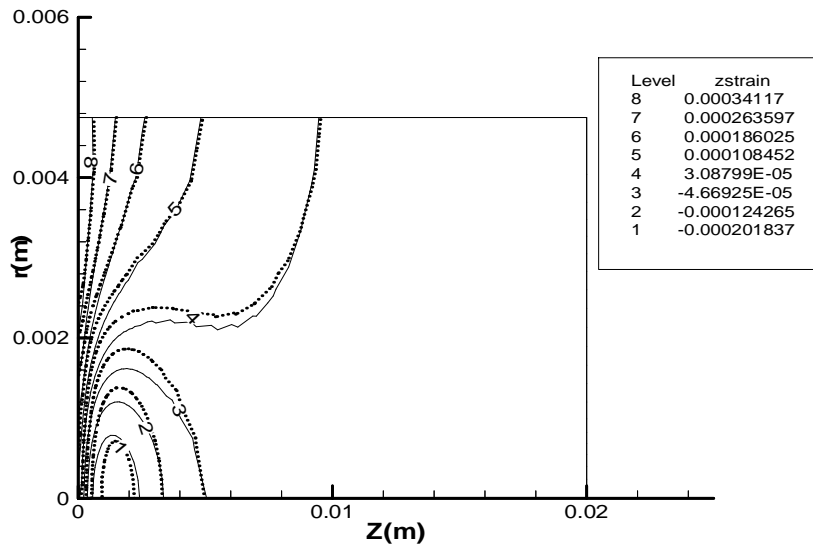


Fig.(5): Longitudinal strain distribution in laser rod in m at absorption power of 100W and radius pumping ratio of 1/2, solid line for Gaussian beam pumping, and the dashed line for Top hat beam pumping.

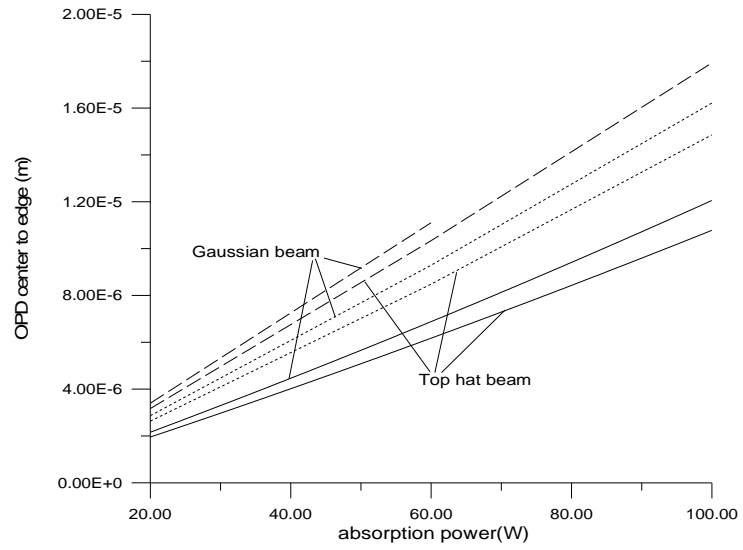


Fig.(6): Variation in OPD with absorption power at different pumping radius, and different pumping beam profile, solid line for pumping radius=1/2,dot line for pumping radius=1/3, dashed line for pumping radius=1/4.

تأثير طرق الضخ على فرق المسار البصري في قضيب ليزر Nd:YAG

زهراء محمد علي كامل

مدرس مساعد

قسم هندسة الليزر والبصريات الالكترونية_الجامعة التكنولوجية

الخلاصة

في هذا البحث تم استعمال طريقة العناصر المحددة لتحديد توزيع درجات الحرارة في قضيب ليزر الـ Nd:YAG المعرض للضخ من احد اطرفه والمبرد طولياً بواسطة الماء. الازاحة الطولية والازاحة القطرية الانفعال والاجهاد الحراريين تم حسابها معتمدا على توزيع درجات الحرارة بالاستناد الى قانون هوك. تأثير طريقتا الضخ الكاوسية والمنتظمة التوزيع خلال قطر الحزمة على توزيع درجات الحرارة، الازاحة والجهد تمت استنباطها ايضا. من هذه الدراسة تم الحصول على قيم لفرق المسار البصري وتم مقارنتها مع النتائج العملية المنشورة سابقا . نستنتج من هذا البحث ان طريقة ضخ الكاوسية تسبب درجة حرارة في وسط ونهاية القضيب اعلى منها في طريقة الضخ المنتظمة التوزيع خلال قطر الحزمة وبالتالي قيمة اعلى بفرق المسار البصري. كذلك فعلى الرغم من ان طريقة الضخ المنتظمة تسبب قيمة اعلى في الاجهاد المحيطى الا انها تسبب قيمة اقل فى فرق المسار البصرى مقارنة بطريقة الضخ الكاوسية وعلية فهى الطريقة الافضل عندما يكون هناك اختيار بين الاثنين وذلك للتاثير البصرى الضار على عمل الجهاز بزيادة فرق المسار البصرى.